

Learning to Slice Wi-Fi Networks: A State-Augmented Primal-Dual Approach

Yiğit Berkay Uslu
University of Pennsylvania
Philadelphia, PA, USA
ybuslu@seas.upenn.edu

Roya Doostnejad
Intel Corporation
Santa Clara, CA, USA
roya.doostnejad@intel.com

Alejandro Ribeiro
University of Pennsylvania
Philadelphia, PA, USA
aribeiro@seas.upenn.edu

Navid NaderiAlizadeh
Duke University
Durham, NC, USA
navid.naderi@duke.edu

Abstract—Network slicing is a key feature in 5G/NG cellular networks that creates customized slices for different service types with various quality-of-service (QoS) requirements, which can achieve service differentiation and guarantee service-level agreement (SLA) for each service type. In Wi-Fi networks, there is limited prior work on slicing, and a potential solution is based on a multi-tenant architecture on a single access point (AP) that dedicates different channels to different slices. In this paper, we define a flexible, constrained learning framework to enable slicing in Wi-Fi networks subject to QoS requirements. We specifically propose an unsupervised learning-based network slicing method that leverages a state-augmented primal-dual algorithm, where a neural network policy is trained offline to optimize a Lagrangian function and the dual variable dynamics are updated online in the execution phase. We show that state augmentation is crucial for generating slicing decisions that meet the ergodic QoS requirements.

Index Terms—Wi-Fi slicing, 5G, QoS, constrained learning, Lagrangian duality, primal-dual, state augmentation.

I. INTRODUCTION

In enterprise settings, it is vital to manage network operations to support multiple use cases with different requirements [1], [2]. In addition, 3GPP includes architectures to integrate Wi-Fi in converged connectivity (5G + Wi-Fi) in enterprise [3]. Network slicing allows an access point (AP) to allocate the network resources across service-level agreement (SLA) categories rather than individually across many users/flows. Defining dynamic slicing in Wi-Fi with guaranteed quality-of-service (QoS), in a similar fashion as 5G, has the potential to provide mechanisms for seamless dynamic traffic steering across licensed and unlicensed networks. Current Wi-Fi slicing solutions are based on a multi-tenant architecture on a single AP by installing different SSIDs [4], [5]. Despite being simple to implement, this method has drawbacks, including the increased overhead for beacon transmission and probe responses by virtual APs, the lack of QoS differentiation inside each SSID slice, and the limitation of association to one slice.

Machine learning approaches are ubiquitous in resource allocation/optimization problems in wireless networks, and there has been growing attention to tackling network slicing problems through learning-based approaches, with reinforcement learning (RL) methods being the most common [6]–[8]. However, prior work analyzing network slicing with constraints

imposed by QoS requirements is relatively scant. For example, in [7], [8], the QoS requirements are taken into account by either (i) directly adding the weighted QoS requirements to the objective, or (ii) using special functions such as log-barrier functions and an unconstrained, penalized aggregate reward, which is optimized using conventional RL algorithms. These approaches generally lack feasibility guarantees—which is partially remedied by projections to feasible policies—and are highly sensitive to suitable selection of penalty weights.

Constraint-aware online deep reinforcement learning (DRL) training is explored in [9] by leveraging Lagrangian primal-dual methods with a proactive baseline switching. Similarly, [10] handles the QoS constraints by reformulating the learning problem in the dual domain, which is then solved via a primal-dual policy gradient algorithm. The primal-dual methods, although effective, do not guarantee convergence to an optimal policy similar to penalized methods.

In this paper, we define a constrained learning framework to enable dynamic network slicing in Wi-Fi. Sections II and III introduce a flexible Wi-Fi network slicing framework and the problem setup. Departing from the aforementioned works, we formulate the network slicing problem as a constrained radio resource management (RRM) optimization problem and develop an unsupervised state-augmented primal-dual algorithm in Section IV. The notion of state augmentation—proposed in [11] for constrained RL and in [12] for wireless resource allocation—incorporates the Lagrangian dual multipliers into the state space similar to a closed-loop feedback system. This results in a practical online algorithm that samples from an optimal policy and exhibits feasibility and near-optimality guarantees, which do not hold for the regularized and conventional primal-dual methods. We demonstrate these attributes of state augmentation in the context of network slicing with ergodic throughput and latency QoS requirements through numerical experiments in Section V.

II. NETWORK SLICING IN WI-FI

A flexible framework is defined to enable slicing in Wi-Fi, allocating resources to assure SLAs, including maximum delay for low-latency (L) and minimum data rate/throughput for high-throughput (H) cases, while maximizing resource units (RU) available to other slices including best-effort (B). The learning-based slicing module collects data from the ongoing

This work has been supported by NSF-Simons MoDL, Award 2031985, NSF AI Institutes program.

traffic and creates, modifies, and removes slices accordingly so that there is minimal impact on traffic and services in other network slices in the same network.

A. Slice ID

Each slice is uniquely identified by its Network Slice ID or Slice type indicator. Both the devices and the network may initiate slice configuration. The device may request to set up a new connection, but the infrastructure may accept or reject the request based on channel conditions, QoS requirements, and available network capacity. The network may also validate if the user has the right to access a network slice. In case the network initiates slice configuration, the device will convey the provided slice ID.

B. Resource Isolation and Management

A key enabler for slicing is the ability to isolate traffic between different slices, for which there are two solutions.

1) *Scheduling Resources in OFDMA*: Each slice is dynamically configured and allocated a certain portion of the frequency band. Applications in the same slice undergo transmission scheduling and are allocated RUs from the assigned bandwidth. In uplink, a trigger-based approach is used to schedule applications in each slice. A minimum RU is allocated to all applications to support legacy devices.

2) *Multi-Link Operation (MLO)*: The MLO process, newly defined in IEEE802.11be, may facilitate device association to all slices and seamless movement across slices. An MLO device may simultaneously connect to multiple slices and support different traffics with different SLAs.

The slicing framework associates each slice with a main link and one or more auxiliary links, in which the slice has a lower priority with respect to the slices that use the link as the main. The slices that have a low priority on a link will be served in that link only if the flows that use it as primary do not occupy all the available resources. This makes the cross-link slicing mechanism adaptive to the load of each slice. The concept of main and auxiliary multi-link for slicing can also be extended to include licensed bands for multi-spectral slicing.

III. NETWORK SLICING MODEL

Consider a wireless network where each access point (AP) is serving $|\mathcal{U}|$ flows, indexed by $i \in \mathcal{U}$, over a W MHz channel. Each flow $i \in \mathcal{U}$ receives data from the application at an average rate $\bar{\mu}_i > 0$, which must be transmitted from the AP to the user device. The performance requirements each flow must meet are dictated by its SLA, and we consider three SLA categories with distinct ergodic QoS requirements: (i) *high-throughput (H)*, (ii) *low-latency (L)*, and (iii) *best-effort (B)*. The high-throughput SLA requirement is a minimum throughput of r_{\min} bps/Hz, while the low-latency SLA requirement is ℓ_{\max} milliseconds of maximum packet delay/latency. We specify no QoS target for the best-effort SLAs. We assume each flow is associated with only one SLA and denote by \mathcal{U}_H , \mathcal{U}_L , and \mathcal{U}_B the disjoint subsets of flows with high-throughput, low-latency, and best-effort SLAs, respectively.

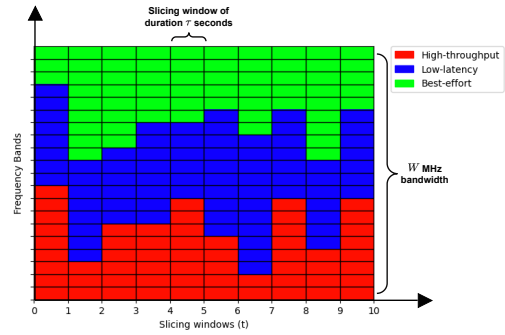


Fig. 1: A network slicing diagram. Frequency subbands are allocated to three types of traffic in each slicing window.

The network operates over T discrete epochs, indexed by $t = 0, \dots, T - 1$. We refer to the discrete epoch t as the t th slicing window. Each slicing window lasts τ_{\max} seconds and we index any timestamp within that slicing window with $\tau \in [0, \tau_{\max})$. Each flow i maintains a queue of size $Q_i^t(\tau) \in [0, Q_{\max}]$ that evolves with a dynamic traffic arrival rate $\alpha_i^t(\tau) \sim \alpha(\bar{\mu}_i^t)$ and a dynamic transmission rate $r_i^t(\tau)$.

The QoS metrics throughput and latency for a flow $i \in \mathcal{U}$ over the t th slicing window, denoted by $\bar{r}_i(t)$ and $\bar{\ell}_i(t)$, respectively, are determined primarily by the dynamic rate $r_i^t(\tau)$ which itself is determined by the frequency resource units (FRUs) allocated to flow i by the AP and the channel state which is an indicator of the signal-to-interference-plus-noise ratio (SINR) experienced by the device receiving flow i . The channel state varies randomly from each slicing window to window, e.g., following a Rayleigh fading channel model.

The goal of a slicing policy is to allocate the FRU resources across SLA categories while ensuring the QoS requirements are satisfied. We represent a slicing decision/policy as

$$\mathbf{p}(t) = (p_H(t), p_L(t), p_B(t))^T, \quad t = 0, \dots, T - 1, \quad (1)$$

where the entries of $\mathbf{p}(t)$ denote the fraction of the total bandwidth allocated to the respective SLA category at the beginning of the slicing window t and all flows associated with the same SLA category access the same slice of resources. For example, if $\mathbf{p}(t) = (1/2, 1/3, 1/6)$ and $W = 20$ MHz, then any high-throughput flow has access to $(1/2) \cdot 20 = 10$ MHz bandwidth. Within each slicing window, the AP further allocates sub-bands at a faster time scale according to some given scheduling algorithm (e.g., round-robin, max-SINR, etc.). Note that the slicing decisions are updated at the beginning of each slicing window. See Fig. 1 for an illustrative diagram.

Due to the dynamic and complex nature of the network traffic, wireless channel conditions, and so on, the network slicing decisions should occur opportunistically across slicing windows and learning-based optimization techniques can be leveraged. Let $\mathbf{s}_t \in \mathcal{S}$ be the overall network state at the beginning of the slicing window t and $\boldsymbol{\theta} \in \Theta \subset \mathbb{R}^d$ be a finite-dimensional (e.g., neural-network) parametrization.

We define the network slicing policy as

$$\mathbf{p}(t) = \mathbf{p}^\theta(\mathbf{s}_t; \boldsymbol{\theta}) \quad (2)$$

that takes the network state \mathbf{s}_t as input and outputs the corresponding slicing decisions. Our goal is to optimize the parameter vector $\boldsymbol{\theta}$ to maximize the system performance subject to the QoS requirements and the total bandwidth budget of $p_H(t) + p_L(t) + p_B(t) \leq 1$. Note that we can drop the total bandwidth budget constraint in subsequent derivations since it holds with equality for any optimal slicing decision and can be implicitly satisfied by the design of the learning architecture (e.g., a softmax layer).

We define the network-slicing optimization problem as

$$\begin{aligned} \min_{\boldsymbol{\theta} \in \Theta} \quad & \frac{1}{T} \sum_{t=0}^{T-1} f_0(\mathbf{s}_t, \mathbf{p}^\theta(\mathbf{s}_t; \boldsymbol{\theta})) \\ \text{subject to} \quad & \frac{1}{T} \sum_{t=0}^{T-1} \mathbf{f}(\mathbf{s}_t, \mathbf{p}^\theta(\mathbf{s}_t; \boldsymbol{\theta})) \leq \mathbf{0}, \end{aligned} \quad (3)$$

where $f_0 : \mathcal{S} \times \mathbb{R}^3 \rightarrow \mathbb{R}$ is the objective (e.g., negated total network throughput), $\mathbf{f} : \mathcal{S} \times \mathbb{R}^3 \rightarrow \mathbb{R}^c$ is the vector-valued constraint function (e.g., minimum throughput and maximum packet latency QoS) for c constraints in total.

The goal of this paper is to develop a learning algorithm to solve (3) for any given network configuration and sequence of network states $\{\mathbf{s}_t\}_{t=0}^{T-1} \in \mathcal{S}$.

IV. PROPOSED STATE-AUGMENTED ALGORITHM

We move to the Lagrangian dual domain and write the Lagrangian function for the parametrized problem as

$$\mathcal{L}(\boldsymbol{\theta}, \boldsymbol{\lambda}) = \frac{1}{T} \sum_{t=0}^{T-1} \left[f_0(\mathbf{s}_t, \mathbf{p}^\theta(\mathbf{s}_t; \boldsymbol{\theta})) + \boldsymbol{\lambda}^\top \mathbf{f}(\mathbf{s}_t, \mathbf{p}^\theta(\mathbf{s}_t; \boldsymbol{\theta})) \right], \quad (4)$$

where $\boldsymbol{\lambda} = (\lambda_1, \dots, \lambda_c)^\top \in \mathbb{R}_+^c$ is the vector of nonnegative dual multipliers corresponding to the QoS constraints. Defining the dual function as $d(\boldsymbol{\lambda}) := \min_{\boldsymbol{\theta} \in \Theta} \mathcal{L}(\boldsymbol{\theta}, \boldsymbol{\lambda})$, the primal and dual problems are related by

$$D_\theta^* := \max_{\boldsymbol{\lambda} \in \mathbb{R}_+^c} d(\boldsymbol{\lambda}) = \max_{\boldsymbol{\lambda} \in \mathbb{R}_+^c} \min_{\boldsymbol{\theta} \in \Theta} \mathcal{L}(\boldsymbol{\theta}, \boldsymbol{\lambda}) \leq P_\theta^* \quad (5)$$

where P_θ^* is the optimum value of parametrized primal problem and $P_\theta^* - D_\theta^*$ is the duality gap. While the duality gap is generally nonzero for the parametrized problem, it becomes sufficiently small as the parametrization becomes richer [13]. More importantly, although both the Lagrangian in (4) and the dual problem (5) are nonconvex in $\boldsymbol{\theta}$, the outer maximization in the latter is a convex problem. In practice, the inner exact minimization corresponding to the primal policy optimization is also replaced by stochastic gradient-descent which results in an iterative primal-dual algorithm given by

$$\begin{aligned} \boldsymbol{\theta}_{k+1} &= \boldsymbol{\theta}_k - \eta_\theta \nabla_{\boldsymbol{\theta}} \mathcal{L}(\boldsymbol{\theta}_k, \boldsymbol{\lambda}_k), \\ \boldsymbol{\lambda}_{k+1} &= \left[\boldsymbol{\lambda}_k + \eta_\lambda \mathbf{f}(\boldsymbol{\theta}_{k+1}) \right]_+, \end{aligned} \quad (6)$$

where $k = 0, 1, \dots$, is an iteration index, η_θ and η_λ are the step sizes for the primal and dual variables, respectively, and $[\cdot]_+ := \max(\cdot, \mathbf{0})$. The trajectories $(\boldsymbol{\theta}_k, \boldsymbol{\lambda}_k)_{k \geq 0}$ generated

by running (6) lead to near-optimal and feasible decisions asymptotically under some mild assumptions [11], [12].

Running primal-dual algorithms online in practice is difficult and stopping the offline training at an arbitrary iteration k does not necessarily guarantee that $\boldsymbol{\theta}_k$ yields a feasible slicing policy. In fact, cyclooscillatory behavior of constraints is a common phenomenon. To remedy these challenges, we resort to a state-augmented parametrization $\phi \in \Phi$, proposed in [11], [12], where the network state \mathbf{s} is *augmented* with the dual multiplier vector $\boldsymbol{\lambda}$ corresponding to the QoS constraints at the slicing window t and we denote the slicing policy as $\mathbf{p}^\phi(\mathbf{s}, \boldsymbol{\lambda}; \phi)$. This way, the dual multipliers, which track the evolution of constraint satisfactions/violations over time, are incorporated into the state space. We define the Lagrangian

$$\begin{aligned} \mathcal{L}_\lambda(\phi) &= \frac{1}{T} \sum_{t=0}^{T-1} \left[f_0(\mathbf{s}_t, \mathbf{p}^\phi(\mathbf{s}_t, \boldsymbol{\lambda}; \phi)) \right. \\ &\quad \left. + \boldsymbol{\lambda}^\top \mathbf{f}(\mathbf{s}_t, \mathbf{p}^\phi(\mathbf{s}_t, \boldsymbol{\lambda}; \phi)) \right]. \end{aligned} \quad (7)$$

An optimal state-augmented parametrization is defined to be a minimizer of the expectation of the Lagrangian w.r.t. a dual multiplier sampling distribution q_λ , i.e.,

$$\phi^* \in \underset{\phi \in \Phi}{\operatorname{argmin}} \mathbb{E}_{\boldsymbol{\lambda} \sim q_\lambda} \mathcal{L}_\lambda(\phi). \quad (8)$$

Given that the learning parameterization is sufficiently expressive (e.g., deep neural networks), the learned optimal state-augmented parameterization ϕ^* approximates the Lagrangian minimizers $\theta^\dagger(\boldsymbol{\lambda}) := \operatorname{argmin}_{\boldsymbol{\theta} \in \Theta} \mathcal{L}_\lambda(\boldsymbol{\theta})$ for any $\boldsymbol{\lambda} \sim q_\lambda$.

The offline training of the state-augmented algorithm solves (8), which in practice can be accomplished by replacing the expectation with training batch averages and minimizing the empirical average Lagrangian using gradient-descent-based approaches. Given a batch of sequences of network states and augmenting dual multipliers $\{\boldsymbol{\lambda}_b, \{\mathbf{s}_{b,t}\}_{t=0}^{T-1}\}_{b=0}^{B-1}$, the empirical Lagrangian is defined as

$$\hat{\mathcal{L}}(\phi_n) := \frac{1}{B} \sum_{b=0}^{B-1} \mathcal{L}_{\boldsymbol{\lambda}_b}(\phi_n), \quad (9)$$

and the state-augmented model parameters are updated as

$$\phi_{n+1} = \phi_n - \eta_\phi \nabla_\phi \hat{\mathcal{L}}(\phi_n). \quad (10)$$

During the online execution phase, we derive the network-slicing decisions using the trained state-augmentation parametrization augmented with the current dual multipliers, and every T_0 slicing windows, dual multipliers are updated proportional to the constraint slacks as

$$\boldsymbol{\lambda}_{k+1} = \left[\boldsymbol{\lambda}_k + \frac{\eta_\lambda}{T_0} \sum_{t=kT_0}^{(k+1)T_0-1} \mathbf{f}(\mathbf{s}_t, \mathbf{p}^\phi(\mathbf{s}_t, \boldsymbol{\lambda}_k; \phi^*)) \right]_+. \quad (11)$$

The training and test phases of the state-augmented algorithm are summarized in Fig. 2. We note that under some mild technical assumptions, near-optimality and almost sure feasibility guarantees of (6) extend to the state-augmented primal-dual algorithm. Moreover, although we do not consider a CRL

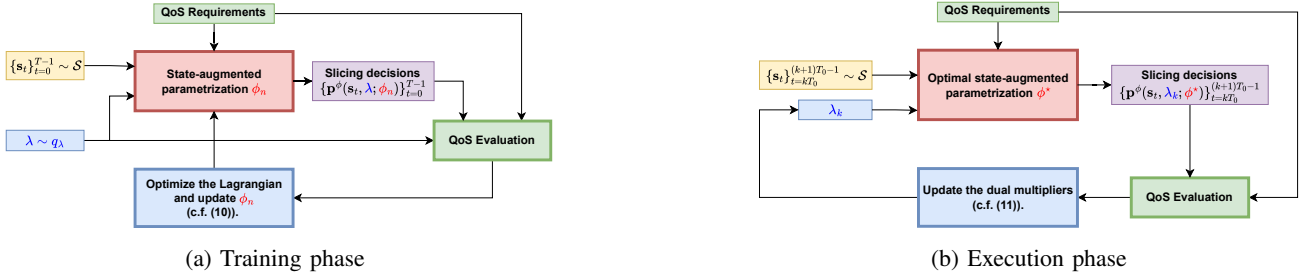


Fig. 2: (a) Offline training, and (b) online execution phases of the proposed state-augmented slicing algorithm.

problem, our proposed algorithm is amenable to tackling CRL problems. We refer the reader to [11], [12] for a theoretical exposition on the state-augmented primal-dual algorithms.

V. EXPERIMENTAL RESULTS

Given a FRU allocation $\mathbf{p}(t)$ and associated channel state $\mathbf{h}^t(\tau)$, we can define the average throughput $\bar{r}_i(t)$ over a slicing period t for each flow i as follows. The instantaneous data rate with a current channel state h and corresponding SINR is given by the Shannon rate $g(h) := \log(1 + h/\sigma^2)$. The full instantaneous rate for flow i can be defined as

$$r_i^t(\tau) = x_i(t) \cdot g(h_i^t(\tau)), \quad (12)$$

where $x_i(t) = \{p_m(t) | i \in \mathcal{U}_m\}$ is the fraction of the total bandwidth W assigned to the SLA category of flow i and the average throughput is given by

$$\bar{r}_i(t) = \overline{r_i^t(\tau)} = \mathbb{E}_{\tau \in [0, \tau_{\max}]} [r_i^t(\tau) \cdot \beta_i^t(\tau)] \quad (13)$$

where $\beta_i^t(\tau)$ evaluates to 1 whenever flow i is scheduled to transmit and has nonempty packet buffer and 0 otherwise. We utilize a uniform round-robin scheduler.

Let the set $\mathcal{J}_i^t = \{j_{i,1}^t, j_{i,2}^t, \dots, j_{i,N_i}^t\}$ denote the transmitted packets of flow i during slicing window t . For a packet $j \in \mathcal{J}_i^t$, we can define the packet latency as

$$\ell_i^t(j) := \frac{\tau_j - \alpha_j}{P} + \frac{1}{r_i^t(\tau_j)P}, \quad (14)$$

where $r_i^t(\tau_j)$ is the instantaneous rate during transmission of packet j as defined in (12), $P > 0$ is the fixed packet size, α_j and τ_j are the arrival and transmission times of packet j , respectively. Then the packet delay is defined as the sum of queuing delay $\tau_j - \alpha_j$ plus the actual transmission delay incurred. We finally define the latency for a given flow over a slicing window as the maximum packet latency, i.e.,

$$\bar{\ell}_i(t) := \max_{j \in \mathcal{J}_i^t} \ell_i^t(j). \quad (15)$$

A. Experimental Setup

The total bandwidth is $W = 20$ MHz. We fix the total number of flows to $|\mathcal{U}| = 20$ and randomly sample the (initial) number of H, L and B flows for each network configuration. Packet generations and traffic arrival for all flows follow a constant bit rate model, mean packet generation rates $\bar{\mu}_i^t$ are (uniform) randomly sampled and dynamic packet generation

rates $\alpha(\bar{\mu}_i^t)$ vary across slicing windows following a random-walk with noise standard deviation of 0.5 bps/Hz. The initial average data rates are sampled randomly $\text{Unif}[1, 5]$ bps/Hz for high-throughput and best-effort flows and $\text{Unif}[0.5, 1.5]$ bps/Hz for the low-latency slices. We adopt the Rayleigh fading channel model and the transmitter and access-point (AP) deployment approach of [12].

We set a minimum throughput requirement of $r_{\min} = 1.0$ bps/Hz for the high-throughput slices and a maximum tail packet latency requirement of $\ell_{\max} = 10$ ms for the low-latency slices. Best-effort slices have no QoS constraints. The network slicing problem with throughput and latency QoS metrics described by (13) and (15), respectively, is mapped to the constrained optimization problem of (3) with state-augmented parametrization as

$$\begin{aligned} \max_{\phi \in \Phi} & \frac{1}{T} \sum_{t=0}^{T-1} \frac{1}{|\mathcal{U}_B|} \sum_{i \in \mathcal{U}_B} \bar{r}_i(\mathbf{s}_t, \mathbf{p}^\phi(\mathbf{s}_t, \boldsymbol{\lambda}_{[t/T_0]}; \phi)) \\ \text{s.t.} & \frac{1}{T} \sum_{t=0}^{T-1} \left[\max_{i \in \mathcal{U}_H} \left(1 - \frac{\bar{r}_i(\mathbf{s}_t, \mathbf{p}^\phi(\mathbf{s}_t, \boldsymbol{\lambda}_{[t/T_0]}; \phi))}{r_{\min}} \right) \right] \leq 0, \\ & \frac{1}{T} \sum_{t=0}^{T-1} \left[\max_{i \in \mathcal{U}_L} \left(\frac{\bar{\ell}_i(\mathbf{s}_t, \mathbf{p}^\phi(\mathbf{s}_t, \boldsymbol{\lambda}_{[t/T_0]}; \phi))}{\ell_{\max}} - 1 \right) \right] \leq 0. \end{aligned} \quad (16)$$

The objective is to maximize the average throughput for best-effort slices. We formulate the QoS constraints as the ergodic average of the worst-case metrics over the respective SLAs to account for varying number of flows.

Slicing decisions are made across $T = 50$ windows and the dual multipliers are updated every $T_0 = 2$ slicing windows during online execution of the state-augmented primal-dual algorithm. At each slicing window, all flows within the same SLA category take turns to transmit their packets to the AP via a round-robin scheduling algorithm, in parallel for all SLA categories. During transmission, the whole subband allocated to the respective slice is utilized by the flows and we assume no interband interference. Although the duration of each slicing window can span several minutes/hours in practice, we simulate and evaluate over slicing windows of duration $\tau_{\max} = 50$ ms for the sake of faster simulations.

For both primal-dual policies, we use multilayer perceptron (MLP) parametrizations with two hidden layers of width 64 followed by a hidden layer of width 32 and a final softmax

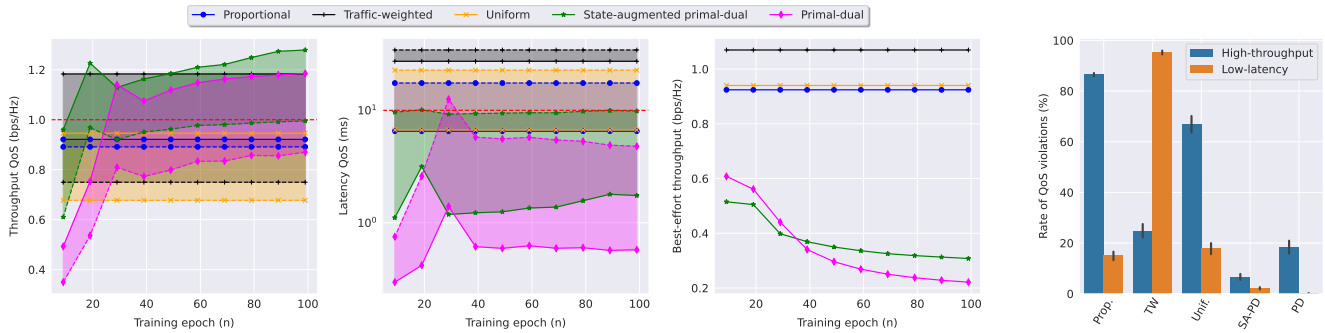


Fig. 3: Test evolutions of high-throughput (left), low-latency (middle-left) QoS constraints, best-effort throughput objective (middle-right) and average rate of QoS violations (right) for the proposed state-augmented primal-dual algorithm and the baselines. Objective and the constraints are averaged (solid lines) over 128 test network realizations and the shadowed bands cover to the worst (99th percentile) realization (dashed lines). Red dashed lines indicate the respective QoS requirements.

layer. The inputs to the models are the concatenation of the network state vector \mathbf{s}_t and the dual multiplier vector $\boldsymbol{\lambda}_{\lfloor t/T_0 \rfloor}$. The output $\mathbf{p}(t)$ is a vector of the fraction of the total bandwidth allocated to the slices. The network state vector at slicing window t is the concatenation of the vector of fraction of flows in each slice and the average and total data rates across each slice, estimated from the previous slicing window.

We train both models over 128 different network configuration for 100 training epochs with a learning rate of 10^{-4} . The augmenting dual multipliers for the state-augmented model are sampled uniformly from $[0, \boldsymbol{\lambda}_{\max}] \times [0, \boldsymbol{\lambda}_{\max}]$ with $\boldsymbol{\lambda}_{\max} = \mathbf{1}$ initially and $\boldsymbol{\lambda}_{\max}$ is updated at the end of each training epoch by running the online dual updates on a validation set of training networks. We test the trained models on 128 network realizations. Dual step size for primal-dual training and online execution of the state-augmented algorithm are set to $\eta_{\boldsymbol{\lambda}}^{PD} = 0.1$ and $\eta_{\boldsymbol{\lambda}} = 1.0$, respectively.

We consider the following traditional slicing baselines:

- *Uniform*: The total bandwidth available is split equally among all slices, i.e., $\mathbf{p} = (1/3, 1/3, 1/3)$ in our setup.
- *Proportional*: The total bandwidth is sliced proportional to the number of active flows in each slice.
- *Traffic-weighted (TW)*: The total bandwidth is sliced proportional to the actual total traffic demand.

B. Simulation Results & Discussion

In Fig. 3, we present the test performance of the primal-dual (PD) and state-augmented primal-dual (SA-PD) algorithms against the baselines. The first three subfigures from the left show the evolution of the test performance of the algorithms with respect to the training epochs. We validate that the state-augmented algorithm meets the throughput and latency QoS requirements while none of the traditional baselines meet the constraints simultaneously. The primal-dual algorithm iterates, although feasible for an average network, do not converge to strictly feasible policies for all networks and constraints simultaneously unlike the state-augmented algorithm. In the rightmost subfigure, we report the average rate of instantaneous

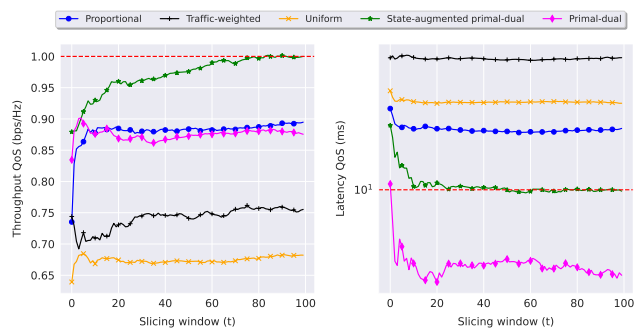


Fig. 4: Time evolution of cumulative ergodic averages of the QoS constraints for the worst realization.

QoS violations and the state-augmented algorithm achieves a low rate of instantaneous violation for both constraints on top of ergodic feasibility. Furthermore, we plot the evolution of the QoS constraints for the worst network realization across slicing windows for fully trained models in Fig. 4 and verify the ergodic feasibility of the state-augmented slicing policy.

In Fig. 5, we illustrate the online execution of the state-augmented algorithm for an example test network. As the throughput constraint is initially violated, the corresponding dual multipliers and the slice weights allocated to high-throughput slices increase until the throughput constraint is met. Fig. 6 exemplifies the policy switching behavior of the state-augmented algorithm where alternating spikes in dual multipliers lead to switching between prioritizing high-throughput and low-latency slices to maintain the feasibility of both constraints. Finally, we report in Table I the average rate of instantaneous and ergodic QoS violations for varying constraint level specifications. An ergodic throughput QoS violation occurs for a flow $i \in \mathcal{U}_H$ whenever $(1/T) \sum_{t=0}^{T-1} \bar{r}_i(t) < r_{\min}$ happens. Ergodic latency violations are defined similarly. Both primal-dual algorithms outperform the traditional baselines and the state-augmented algorithm generally attains comparable, if not better, ergodic QoS satisfaction.

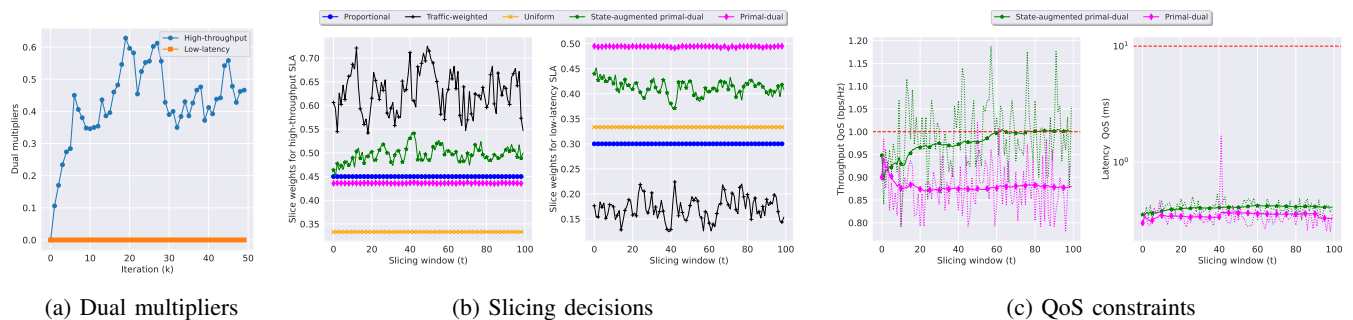


Fig. 5: Time evolution of (a) dual multipliers, (b) slicing decisions and (c) instantaneous (dotted) and average (solid) constraints over slicing windows for an example test network. Constraint averages are computed over a sliding window of length $T = 50$.

TABLE I: Comparison of Rate of Instantaneous and Ergodic QoS Violations

r_{\min} (bps/Hz)	ℓ_{\max} (ms)	High-throughput average instantaneous and ergodic QoS violations (%)					Low-latency average instantaneous and ergodic QoS violations (%)				
		Proportional	T.W.	Uniform	SA-PD	PD	Proportional	T.W.	Uniform	SA-PD	PD
0.7	5	0.3	1.6	7.6	1.5	6.0	27.5	98.5	35.6	0.4	0.3
		0.3	0.1	0.1	0.9	4.7	25.3	99.9	35.5	0.1	0.1
0.9	10	30.7	13.5	42.0	1.8	2.5	14.9	95.4	18.1	4.0	1.3
		2.2	0.1	56.2	0.1	2.0	13.1	98.4	16.1	1.2	0.7
0.9	20	30.7	13.5	42.0	0.1	2.6	0.5	73.5	1.8	3.8	1.2
		2.5	9.4	56.2	0.1	1.6	0.1	76.3	1.0	0.3	0.6
1.0	10	86.6	24.8	66.9	6.6	18.3	15.0	95.2	17.8	2.1	0.2
		99.9	18.0	56.2	3.8	18.0	13.0	98.3	15.8	0.2	0.1

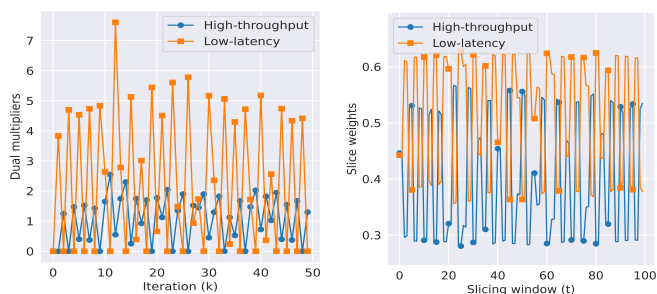


Fig. 6: Example of policy switching with state-augmentation.

VI. CONCLUSION AND FUTURE WORK

We formulated (Wi-Fi) network slicing as a constrained learning problem. Through numerical simulations, we illustrated that a state-augmented algorithm that minimizes an expected Lagrangian offline and updates the dual multipliers online lends itself to a practical primal-dual algorithm with feasibility and optimality guarantees for network slicing. Extension to a state-augmented RL algorithm for network slicing and end-to-end evaluation on a more realistic simulation platform are interesting future research directions.

REFERENCES

- [1] Xuemin Shen, Jie Gao, Wen Wu, Kangjia Lyu, Mushu Li, Weihua Zhuang, Xu Li, and Jaya Rao, "AI-assisted network-slicing based next-generation wireless networks," *IEEE Open Journal of Vehicular Technology*, vol. 1, pp. 45–66, 2020.
- [2] Wen Wu, Conghao Zhou, Mushu Li, Huaqing Wu, Haibo Zhou, Ning Zhang, Xuemin Sherman Shen, and Weihua Zhuang, "AI-native network slicing for 6G networks," *IEEE Wireless Communications*, vol. 29, no. 1, pp. 96–103, 2022.
- [3] Mario Teixeira Lemes, Antonio Marcos Alberti, Cristiano Bonato Both, Antonio Carlos De Oliveira Júnior, and Kleber Vieira Cardoso, "A tutorial on trusted and untrusted non-3GPP accesses in 5G systems—first steps toward a unified communications infrastructure," *IEEE Access*, vol. 10, pp. 116662–116685, 2022.
- [4] Matteo Nerini and David Palma, "5G network slicing for Wi-Fi networks," in *2021 IFIP/IEEE International Symposium on Integrated Network Management (IM)*. IEEE, 2021, pp. 633–637.
- [5] WB Alliance, "Network slicing: Understanding Wi-Fi capabilities," Tech. Rep., March 2018.
- [6] Mohammad Zangoeei, Niloy Saha, Morteza Golkarifard, and Raouf Boutaba, "Reinforcement learning for radio resource management in RAN slicing: A survey," *IEEE Communications Magazine*, vol. 61, no. 2, pp. 118–124, 2023.
- [7] Kun Yang, Shu ping Yeh, Menglei Zhang, Jerry Sydir, Jing Yang, and Cong Shen, "Advancing RAN slicing with offline reinforcement learning," 2023.
- [8] Yongshuai Liu, Jiaxin Ding, and Xin Liu, "A constrained reinforcement learning based approach for network slicing," in *2020 IEEE 28th International Conference on Network Protocols (ICNP)*. IEEE, 2020, pp. 1–6.
- [9] Qiang Liu, Nakjung Choi, and Tao Han, "Onslicing: online end-to-end network slicing with reinforcement learning," in *Proceedings of the 17th International Conference on emerging Networking Experiments and Technologies*, 2021, pp. 141–153.
- [10] Patrick Agostini, Ehsan Tohidi, Martin Kasparick, and Sławomir Stańczak, "Learning constrained network slicing policies for industrial applications," in *2022 IEEE International Conference on Communications Workshops (ICC Workshops)*. IEEE, 2022, pp. 1–6.
- [11] Miguel Calvo-Fullana, Santiago Paternain, Luiz Chamon, and Alejandro Ribeiro, "State augmented constrained reinforcement learning: Overcoming the limitations of learning with rewards," *IEEE Transactions on Automatic Control*, vol. PP, pp. 1–15, 01 2023.
- [12] Navid NaderiAlizadeh, Mark Eisen, and Alejandro Ribeiro, "State-augmented learnable algorithms for resource management in wireless networks," *IEEE Transactions on Signal Processing*, 2022.
- [13] Santiago Paternain, Luiz Chamon, Miguel Calvo-Fullana, and Alejandro Ribeiro, "Constrained reinforcement learning has zero duality gap," in *Advances in Neural Information Processing Systems*, H. Wallach, H. Larochelle, A. Beygelzimer, F. d'Alché-Buc, E. Fox, and R. Garnett, Eds., 2019, vol. 32.